Geophysical Research Letters

RESEARCH LETTER
10.1029/2024GL114398

Disagreement in Detected Heatwave Trends Resulting From Diagnostic Methods

Boyuan Zhang[1], Yongli He[1,2], Zhanbo Wang[1], Bo Huang[1], Yongkun Xie[2], Xiaodan Guan[1,2], and Jianping Huang[1,2]

[1]Key Laboratory for Semi-Arid Climate Change of the Ministry of Education, School of Atmospheric Sciences, Lanzhou University, Lanzhou, China, [2]Collaborative Innovation Center for Western Ecological Safety, Lanzhou, China

Key Points:

- Heatwave metrics exhibit high sensitivity to parameter selection in the 3-dimensional connected detection algorithm
- Parameters with 40%–50% overlap, 10^6 km^2 area threshold, and 10-connected structure are suitable for identifying large-scale heatwaves
- Significant increases in heatwave frequency, projection area and total magnitude were observed from 1959 to 2023

Supporting Information:

Supporting Information may be found in the online version of this article.

Correspondence to:

Y. He,
heyongli@lzu.edu.cn

Citation:

Zhang, B., He, Y., Wang, Z., Huang, B., Xie, Y., Guan, X., & Huang, J. (2025). Disagreement in detected heatwave trends resulting from diagnostic methods. *Geophysical Research Letters*, *52*, e2024GL114398. https://doi.org/10.1029/2024GL114398

Received 19 DEC 2024
Accepted 3 MAR 2025

Author Contributions:

Conceptualization: Boyuan Zhang, Yongli He
Formal analysis: Boyuan Zhang, Yongli He, Zhanbo Wang, Bo Huang
Funding acquisition: Yongli He, Xiaodan Guan
Investigation: Boyuan Zhang, Yongkun Xie
Methodology: Boyuan Zhang, Yongli He
Project administration: Yongli He
Software: Zhanbo Wang
Supervision: Yongli He
Writing – original draft: Boyuan Zhang

Abstract Heatwaves pose increased risk to ecosystem and society. Advanced event-based detection methods offer novel insights into the spatiotemporal dynamics of heatwaves. However, robust assessments of heatwave trends remain challenging due to the sensitivity of results to parameter selection, including connected structure, area threshold, and overlap ratio. Here, we employed 3-dimensional connected detection algorithm (3DCDA) to explore the dependency of heatwave identifications on various parameter combinations. The results indicate that heatwave metrics are sensitive to 3DCDA parameters, with the appropriate combination for large-scale heatwaves being overlap ratio of 40%–50%, area threshold of 10^6 km^2, and 10-connected structure. Based on this configuration, we discovered significant increasing trends in heatwave frequency, projection area and total magnitude, while observed a decrease in maximum intensity and area mean intensity both annually and during summer. These findings highlight the critical importance of parameter selection in 3DCDA for robust analysis of heatwaves and other extreme events.

Plain Language Summary Heatwaves pose serious threats to ecosystem and society. Understanding how heatwaves evolve is important. Previous studies have primarily examined heatwave evolution at individual grids, neglecting the propagation of heatwaves across neighboring regions. Although recent research has recognized this phenomenon, the utilization of different detection methods has led to inconsistent results. To address this issue, we first use the 2021 Northwestern Pacific Heatwave as a case study. Our findings indicate that an excessively high overlap ratio only captures the peak stage of the heatwave, while an excessively low overlap would merge unconnected heatwaves into an event. We then examined all heatwaves from 1959 to 2023 and ultimately recommended the following criteria for large-scale heatwaves: the affected region should overlap by 40%–50% from one day to the next, the coverage area should be larger than 10^6 km^2, and the analysis should consider both neighboring regions on the same day and closely connected regions across consecutive days. Applying these parameters, we discover increasing trends in heatwave frequency, areal coverage and total magnitude. These results highlight the importance of carefully selecting parameters in the 3DCDA, which can also serve as a valuable reference for identifying other types of extreme events.

1. Introduction

Heatwaves, defined as periods of extreme high temperature lasting more than three consecutive days, have profound impacts on labor productivity (Zander et al., 2015), human health (Xu et al., 2016; Ye et al., 2012), public infrastructure (McEvoy et al., 2012; Rübbelke & Vögele, 2011) and the economy (Kjellstrom, 2015; Tang et al., 2023). The frequency, intensity, and formation mechanisms of heatwaves have been extensively studied at both global and regional scales (Kornhuber et al., 2019, 2020; Perkins, 2015; Perkins et al., 2012; Rousi et al., 2022). However, these studies focus on individual grid points, overlooking the spatiotemporal continuity of heatwaves by reducing the three-dimensional (time × latitude × longitude) attributes to one or two dimensions. This reduction limits a comprehensive understanding of their spatiotemporal evolution.

To address the spatiotemporal dynamics of heatwaves, various algorithms have been developed to characterize heatwave metrics (He et al., 2023; Liu & Zhou, 2023; Lyon et al., 2019; Song et al., 2022; Vogel et al., 2020; Wu et al., 2024). One approach clusters two-dimensional latitude–longitude grid points and subsequently utilizes an overlap ratio to merge or split extreme events (Fang & Lu, 2020; Kong et al., 2024; Wang & Wang, 2023). Another approach directly identifies events in three-dimensional spatiotemporal space and applies specific rules for event identification (Luo et al., 2022; X. Wang, Luo, et al., 2022). For example, utilizing the 3D connected component algorithm (CC3D), researchers have identified 3D heatwave events both regionally and globally (Luo

Writing – review & editing:
Boyuan Zhang, Yongli He, Zhanbo Wang, Bo Huang, Yongkun Xie, Xiaodan Guan, Jianping Huang

et al., 2022, 2024; Wu et al., 2024). Recently, with the emergence of machine learning algorithms, Liu et al. (2023) utilized 3D-DBSCAN to identify the 2022 heatwave in the Yangtze River Basin and explore the sensitivity of parameter selection in this algorithm. However, the physical relevance of parameter choice in such algorithms remains inadequately explored.

Careful parameter selection is crucial for implementing the three-dimensional connected detection algorithm (3DCDA), as different parameters can lead to significant variations in the results (Song et al., 2022; Vogel et al., 2020). For example, the choice of fixed or moving thresholds significantly influences heatwave attributes (Vogel et al., 2020). Similarly, overlap ratios are critical for ensuring spatial continuity in event detection (Li et al., 2020). Studies have reported varying overlap ratios and resolutions for different extreme events, such as a 50% overlap ratio with a 3.75° × 2.5° resolution for heatwaves (C. Wang, Zheng, et al., 2022) and a 70% overlap ratio with a 1° × 1° resolution for atmospheric blocking (Pfahl et al., 2015; Steinfeld & Pfahl, 2019), highlighting the need to investigate its impact on event identification. Furthermore, different connected structures can yield varying outcomes in heatwave detection (He et al., 2023). By setting a 250-km buffering zone at land boundaries, minimal differences of heatwave characteristics are detected when ocean areas were included compared to land-only analyses (Luo et al., 2024). However, Lo et al. (2021) cautioned that focusing solely on land could underestimate heatwave size in island and coastal regions. To address these complexities, this study compares heatwave identification at global and land-only scales to assess the influence of spatial scale on heatwave detection. Understanding the sensitivity of parameter selection in the 3DCDA is crucial for investigating the response of heatwaves and other extreme events to global warming.

This study provides a comprehensive assessment of parameter dependency in 3DCDA using the ERA5 data set. First, we conducted sensitivity experiments using the 2021 Northwestern Pacific heatwave as a case study (Oertel et al., 2023; Schumacher et al., 2022). Subsequently, we extended these sensitivity experiments to analyze global heatwave events from 1959 to 2023. Different parameter combinations can be used to identify various types of heatwaves. Small-scale heatwave are often influenced by regional factors such as urbanization and land-use changes, whereas large-scale contiguous heatwaves are primarily driven by atmosphere circulation. This study focuses on large-scale contiguous heatwaves, as atmosphere circulation can induce more extensive and intense extreme temperature events compared to regional factors. To systematically assess their response to global warming, we employ a specific parameter combination, including a 40%–50% overlap ratio, a minimum projection area of 10^6 km^2 and a 10-connected structure. This analysis not only enhances our understanding of heatwaves but also serves as a valuable reference for studying the spatiotemporal dynamics of other extreme events, such as extreme precipitation, droughts, sandstorms and so on.

2. Methods

2.1. Surface Temperature Data

The surface temperature data used in this study is derived from the European Center for Medium-Range Weather Forecasts (ECMWF) reanalysis (ERA5) data set, covering the period from 1959 to 2023 with spatial resolutions of 1° × 1° and 2.5° × 2.5°, which can be downloaded using the "grid" parameter (Hersbach et al., 2023). Although ERA5 provides a higher native resolution of 0.25°, we use two coarse resolutions in this study, as they are sufficient for analyzing synoptic-scale heatwaves while optimizing computational efficiency. Daily maximum temperature (T_{max}) is derived by calculating the highest temperature from hourly ERA5 data for subsequent analyses.

2.2. Heatwave Definition and 3D-Connected Detection Algorithm

Unlike traditional detection algorithms that identify heatwaves over isolated grids and disregard the spatiotemporal continuity of heatwave events, a 3D-connected detection algorithm (3DCDA) was developed to address these limitations (Figure S1 in Supporting Information S1). The algorithm involves the following steps: (a) Threshold identification: Tmax is used for heatwave detection. The threshold for extreme temperature is set at the 90th percentile of a centered 15-day temporal window of Tmax from 1959 to 2023. (b) Connection determination: For each day, regions where the two-dimensional temperature field exceeds the threshold and is contiguous with neighboring grids are identified as heatwave areas. (c) Overlap Limit: Heatwave areas are preserved only if the overlap area between adjacent days exceeds a specified overlap ratio; otherwise, they are excluded. (d) Persistence Limit: After applying the overlap limit, events are identified using either a 10-connected structure or a 26-

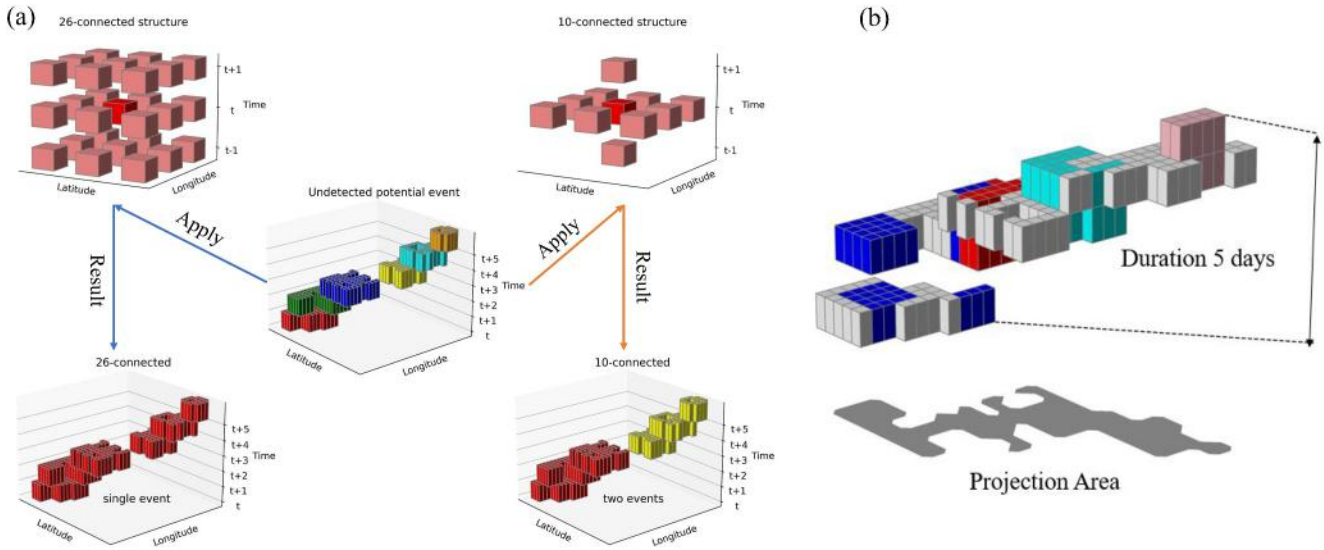

Figure 1. Introduction of the 26-connected structure, 10-connected structure, overlap, duration and projection area. Panel (a) illustrates the difference between the final results for the 10-connected structure and the 26-connected structure. The different colors in panel (b) indicate the overlap area on different days, the bottom shadow represents the projected area, and the arrow on the left signifies the duration.

connected structure (Figure 1a). Only heatwave events persisting for more than 3 days are preserved (Figure 1b). (e) Area Limit: Following the persistence limit, events are further processed based on an area threshold (Figure 1b). If the event spans an area exceeding a certain threshold, it is retained; otherwise, it is eliminated. (f) Metric Diagnosis: Finally, heatwave metrics are determined, including duration, intensity properties, mobility properties, and areal properties (Table S1 in Supporting Information S1). These steps ensure comprehensive and accurate identification of heatwaves while accounting for their spatiotemporal continuity.

2.3. Sensitivity Experiments of the 3DCDA

To evaluate the robustness of the 3DCDA, sensitivity experiments were conducted to assess its performance under varying conditions, including resolutions, spatial scales, connected structures, area thresholds, and overlap ratios, both annually and during the summer season. Summer is defined as June to August in the Northern Hemisphere and December to February in the Southern Hemisphere (Bathiany et al., 2018; Vogt et al., 2022). While previous studies have primarily focused on heatwaves over land (Luo et al., 2022, 2024), the evolution of heatwaves over oceans remains underexplored (King & Reeder, 2021). To address this gap, we compared results on a global scale, including both land and ocean areas, with those confined to land areas. For a precise comparison, heatwave center positions located on land were extracted from the global-scale data. Additionally, the algorithm's stability was examined with spatial resolutions of 1° and 2.5°.

2.3.1. Connected Structure Sensitivity

The choice of connected structure significantly affects the identification of heatwave events. A 10-connected structure tends to segment a potential heatwave event into multiple smaller events, while a 26-connected structure categorizes it as a single, cohesive event (Figure 1a). Given the stricter constraints imposed by the 10-connected structure, it is critical to understand its sensitivity in comparison to the 26-connected structure.

2.3.2. Overlap Ratio Sensitivity

The overlap ratio is another key parameter that affects the identification of extreme events. Variation in the overlap ratio can lead to different outcomes in heatwave detection (Figure 2). The overlap ratio must balance the atmospheric flow's influence and the spatiotemporal continuity of heatwaves. To evaluate its sensitivity, overlap ratios ranging from 0% to 100% were tested using the 2021 Northwestern Pacific Heatwave as a case study.

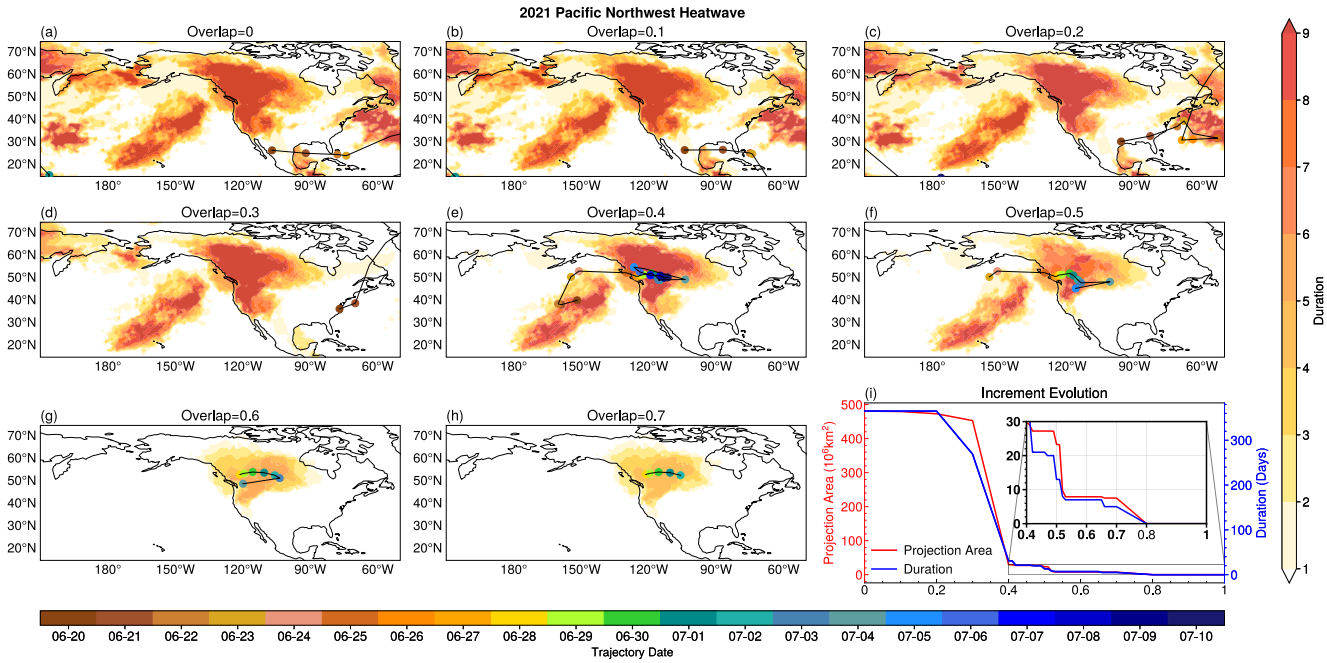

Figure 2. The sensitivity of heatwave duration and projection area to variations in overlap ratios. Panels (a–h) illustrate the spatial distribution of heatwave duration for overlap ratios ranging of 0%–70%, where the filled contours indicate the duration of heatwaves from 20 June 2021, to 10 July 2021, and the black line represents the heatwave trajectory. Circular markers with a brown-to-blue color gradient indicate the progression of time. Panel (i) shows the changes in projection area and duration with increasing overlap ratio, with the red line indicating the projection area and the blue line representing the duration.

2.3.3. Area Threshold Sensitivity

To assess the impact of atmospheric circulation on heatwave evolution, experiments were conducted using area thresholds of 10^6 km^2 (Barriopedro et al., 2011, 2023) and 0 km^2. Smaller heatwaves are often more influenced by local factors than large-scale atmospheric circulation, whereas an area of 10^6 km^2 is equivalent to a circle with a radius of a Rossby wavelength (Osychny & Cornillon, 2004), providing a benchmark for analyzing the effects of atmospheric circulation.

2.3.4. Resolution Comparison

Sensitivity experiments were conducted at spatial resolutions of $1° \times 1°$ and $2.5° \times 2.5°$ to validate the algorithm's consistency across different resolutions.

Further details on these sensitivity experiments are provided in Figure 3 and Figure S8 in Supporting Information S1. These experiments highlight the importance of parameter choices in 3DCDA for accurately capturing the spatiotemporal dynamics of heatwaves.

3. Results

3.1. The Critical Parameters in the 3DCDA

We developed a 3DCDA to identify spatiotemporally continuous heatwaves. According to this algorithm, a heatwave is identified when it overlaps with adjacent days, persist for more than 3 days and covers an area exceeding a specified threshold. The connected structure in this algorithm ensures that a heatwave occurring on a given day can propagate to adjacent regions on subsequent days (Figure 1a). Specifically, a 26-connected structure categorizes potential events as a single heatwave event, whereas a 10-connected structure may split the same potential event into two distinct heatwave events. The overlap ratio further guarantees the spatiotemporal continuity of heatwaves, preventing different events from overlapping or intersecting within the "latitude × longitude × time" space (Figure 1b). The persistence and coverage area of heatwaves serve as critical indices for assessing their impacts at global and regional scales. Additionally, the total magnitude of a heatwave,

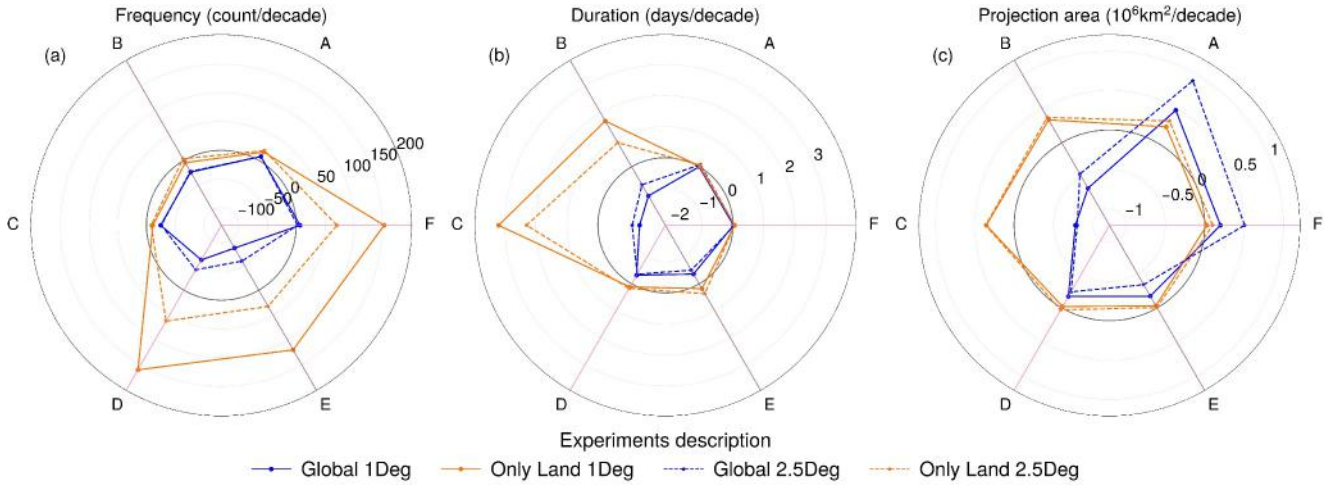

	A	B	C	D	E	F
Overlap (%)	50	0	0	0	0	50
Area (10^6km^2)	1	1	1	0	0	0
Connected structure	10	10	26	10	26	10

Figure 3. Trends of the annual heatwave frequency (a), duration (b) and projection area (c) in the sensitivity experiments. The blue line represents the global scale, and the orange line represents the land-only scale. The solid line represents a resolution of 1°, and the dashed line represents a resolution of 2.5°.

represented as the sum of temperature anomalies across heatwave days and areas, provides a concise metric for quantifying its overall intensity, duration and extent.

3.2. A Case Study of the 2021 Northwest Pacific Heatwave

To evaluate the influence of overlap ratios on heatwave detection, we analyzed the 2021 northwestern Pacific heatwave, an event that broke local historical records and caused substantial ecosystem damage (C. Wang, Zheng, et al., 2022; Lin et al., 2022; White et al., 2023). A 10-connected structure was employed with overlap ratios ranging from 0% to 100% to detect heatwaves globally from 1 January 2021, to 31 December 2021 (Figure 2). A focused analysis was conducted for the period from June 20 to 10 July 2021. When the overlap ratio was below 20%, the algorithm produces unsatisfactory results, incorrectly identifying spatially disconnected regions as a single event. This led to implausible outcomes, such as heatwaves covering an area of approximately 500×10^6 km^2 and persisting for 365 days (Figures 2a–2c and 2i). As the overlap ratio increased from 30% to 50%, the projection area and the duration of the detected heatwaves decreased to approximately 10×10^6 km^2 and 10 days, respectively, yielding more realistic results (Figures 2d–2f and 2i).

The incremental evolution curve of the projection area and duration in response to the overlap ratios revealed that both metrics gradually decreased as the overlap ratio increased, with no heatwave detections beyond 80% (Figure 2i). Specifically, the projection area and duration remained stable from 0% to 20%, sharply decreased from 20% to 40%, and exhibited minor fluctuations from 40% to 50% and 50%–70% (Figure 2i). An overlap ratio below 40% tended to erroneously classify spatially disconnected regions as a single event, whereas ratios above 50% suggested a quasi-stationary state of heatwaves (Figure 2i). Based on these findings, an overlap ratio of 40%–50% was deemed appropriate for effectively capturing the development of large-scale contiguous heatwaves. Compared to the global scale, the land-only scale only identified the peak stage of the heatwave and failed to recognize its onset stage over the ocean (Figures S2 and S3 in Supporting Information S1). Additionally, the choice between 10-connected and 26-connected structures had minimal impact on heatwave evolution, with minor variations in genesis location observed between June 21 and June 22 (Figures S2a and S2b in Supporting Information S1). This analysis highlights the importance of selecting appropriate parameters in heatwave detection algorithms, as the appropriate parameter enhances the reliability of heatwave identification and provides a more accurate depiction of their spatiotemporal dynamics.

3.3. Sensitivity Experiments With Different Parameters of 3DCDA for Global Heatwaves

Building on the findings from the 2021 Northwestern Pacific Heatwave (Figures S2 and S3 in Supporting Information S1), the analysis of heatwaves from 1959 to 2023 revealed consistent probability distribution of heatwave duration and projection area across different connected structures, both annually (Figures S4 and S5 in Supporting Information S1) and during summer (Figures S6 and S7 in Supporting Information S1). This consistency indicates that the choice of connected structure does not significantly impact the distribution of these metrics (Figures S4–S7 in Supporting Information S1). However, significant differences between the probability distributions at the land-only scale and the global scale highlight the importance of including ocean regions in such analyses.

To further explore parameter sensitivity, we compare heatwave metrics across various experimental setups (Figure 3 and Figure S8 in Supporting Information S1). Experiment *A* is conducted with an overlap ratio of 50%, an area threshold of 10^6 km^2, and a 10-connected structure, but experiment *B* and *C* are conducted without overlap limit using a 10-connected structure and a 26-connected structure. Experiment *D* and *E* do not consider the area threshold, potentially allowing for the detection of smaller events compared to experiments *B* and *C*. Experiment *F* also does not consider the area threshold but considers the effect of overlap.

As regional warming intensifies, previously isolated heatwaves are becoming interconnected, leading to a decrease in heatwave frequency but an increase in both duration and projection area at land-only scale when the overlap limit is not applied (Experiments *B* and *C* in Figure 3 and Figure S8 in Supporting Information S1). In contrast, when the overlap limit is considered, both heatwave frequency and projection area exhibit a consistent increase, while duration exhibit minor variations at both global and land-only scales (Experiments *A* and *F*). This suggests that global warming is driving more contiguous heatwaves, affecting a larger spatial extent but not necessarily extending their duration (Figure 3 and Figure S8 in Supporting Information S1).

Localize warming leads to an increase in small-scale heatwaves when the area threshold is removed (Experiments *D* and *E* in Figure 3a and Figure S8a in Supporting Information S1). This is further confirmed by the relatively minor variations in heatwave projection area and duration in experiments with area limits compared to experiments without area limits. Specifically, the increase in these small-area, short-duration heatwaves leads to minor variation of heatwave duration and projection area in Experiments *D* and *E*, while larger-scale heatwaves show an increasing trend in both duration and projection area in Experiments *B* and *C* (Figures 3b and 3c and Figures S8b and S8c in Supporting Information S1).

These findings underscore the critical role of the parameter selection in heatwave detection. The area limit effectively filters out smaller, localized heatwave, while the overlap ratio limit prevents the merging of unrelated heatwaves on a global scale. Despite using the identical experiment configurations, heatwaves exhibit distinct trends at global and land-only scales. Therefore, the parameters selection of 3DCDA should be based on the type of heatwaves (e.g., fast-moving, large-scale and so on).

3.4. Trends in Large-Scale Contiguous Heatwaves

We focus on large-scale contiguous heatwaves due to their high impact. Using the appropriate parameter combination of a 50% overlap ratio, an area threshold of 10^6 km^2, and a 10-connected structure, global large-scale heatwaves were identified based on ERA5 data set both annually (Figure 4) and during summer (Figure S9 in Supporting Information S1). The results revealed extensive regions experiencing significant heatwave impacts, predominately in the high latitudes of the Northern Hemisphere. In contrast, heatwaves in the Southern Hemisphere typically covered smaller areas, less than 10×10^6 km^2, with total magnitudes below 20×10^6°C km^2 (Figure 4a).

The frequency of heatwaves nearly doubled between 1959 and 2023, increasing at a rate of 7.71 events/decade annually and 2.32 events/decade during summer (Figure 4b and Figure S9b in Supporting Information S1). However, the duration of heatwaves exhibits an insignificant trend of −0.003 days/decade annually and 0.08 days/decade during summer (Figure 4c and Figure S9c in Supporting Information S1). Projection area showed a significant increase with the rates of 0.48×10^6 km^2 per decade annually and 0.5×10^6 km^2 per decade during summer (Figure 4d and Figure S9d in Supporting Information S1). Consequently, the total magnitude of heatwaves increases significantly by approximately 5.98×10^6 km^2 °C/decade annually and 6.43×10^6 km^2 °C/decade during summer (Figure 4g and Figure S9g in Supporting Information S1). By contrast, the average

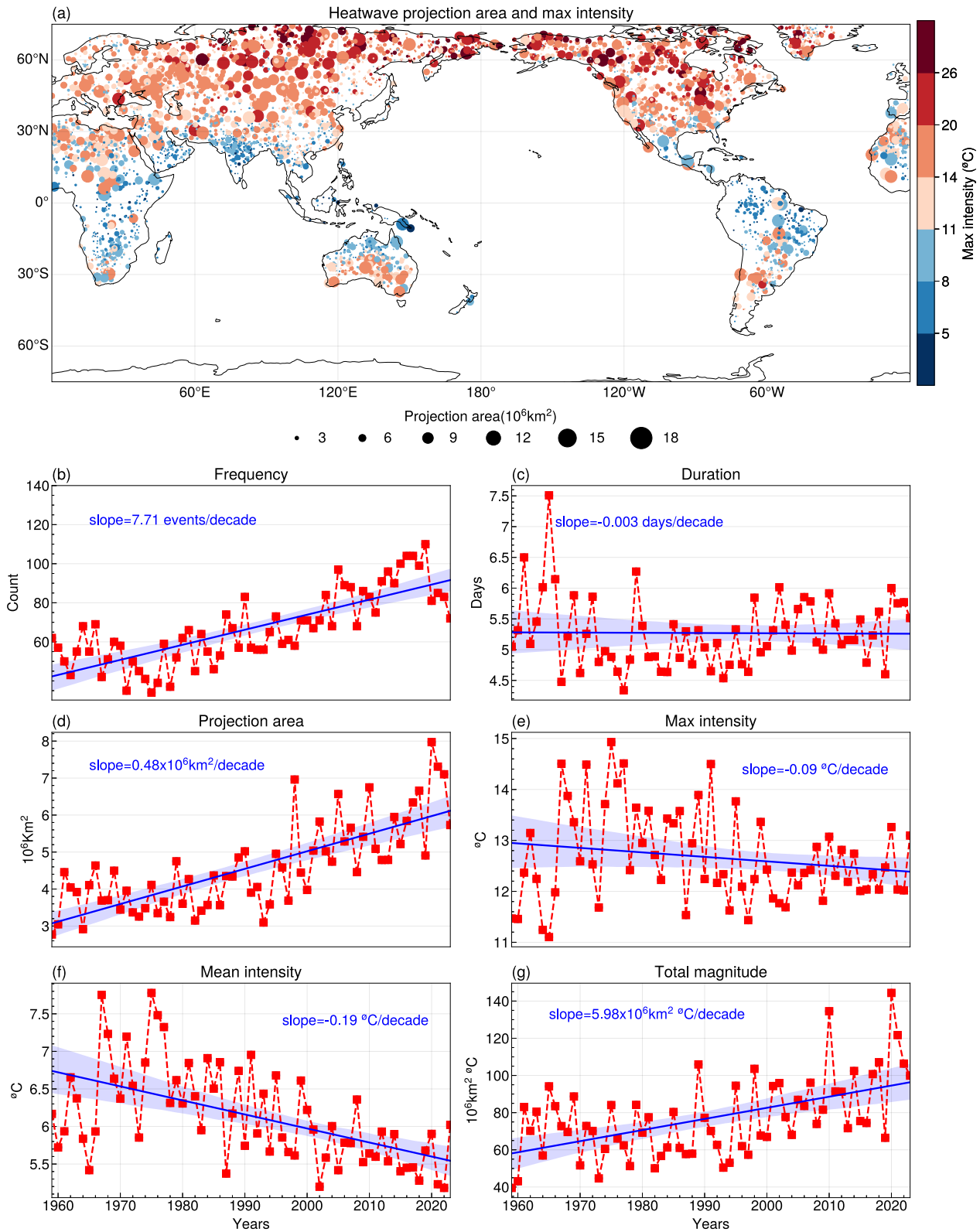

Figure 4. Global annual heatwave properties. (a) The distribution of the centroids of heatwaves spanning from 1959 to 2023, where the color and size of the dots represent the maximum intensity and projection area, respectively. (b)–(g) Time series of heatwave frequency, duration, projection area, maximum intensity, area mean intensity and total magnitude. The blue lines indicate the corresponding linear trends, while the shaded area signifies the 95% confidence interval of the trend line.

maximum intensity of heatwaves exhibited an insignificant change, declining by approximately −0.09°C/decade annually and −0.02°C/decade during summer (Figure 4e and Figure S9e in Supporting Information S1), whereas the most severe heatwaves are becoming more intense, as evidenced by the increasing trend in the annually highest recorded heatwave maximum intensity (Figure S10 in Supporting Information S1). This decline in the average intensity can be attributed to the occurrence of heatwaves in historically less affected regions, which typically experience lower intensity compared to traditional heatwave-prone regions. Meanwhile, the area-mean intensity decreases significantly with rates of −0.19°C/decade annually and −0.17°C/decade during summer (Figure 4f and Figure S9f in Supporting Information S1). This decrease is primarily driven by the spatial expansion of heatwaves, which incorporates regions with lower temperature anomalies, thereby reducing the overall intensity when averaged across the entire affected region. Unlike the increasing heatwave duration reported by Luo et al. (2022), our results indicate minimal changes in heatwave duration, which is consistent with the stable duration of large-scale atmospheric circulation patterns such as atmospheric blocking. This finding underscores the critical importance of selecting appropriate parameters for heatwave detection. Moreover, the significant changes in heatwave characteristics over the past several decades, reflecting the complex responses of heatwaves to global warming.

4. Discussion and Conclusions

Several studies have emphasized the need for a standardized definition and comprehensive assessment of heatwave characteristics (Perkins & Alexander, 2013; Perkins-Kirkpatrick & Lewis, 2020; E. Russo & Domeisen, 2023). Despite these efforts, a wide range of methodologies continue to be used, and a systematic comparative analysis of these methods remains largely absent. This study represents the first comprehensive global analysis of heatwave characteristics employing the 3DCDA across various experimental setups. Our findings demonstrate that parameter selection significantly influences the identification of large-scale contiguous heatwave. Using a parameter combination of a 50% overlap ratio, an area threshold of 10^6 km^2, and a 10-connect structure for the 3DCDA, we observed significant increases in heatwave frequency, projection area and total magnitude annually and during summer (Figure 4 and Figure S9 in Supporting Information S1). The following are key findings of the study:

1. Land-only versus Global scale analyses:
   It is not possible to artificially separate the evolution of heatwave over the ocean and land. Specifically, land-only analysis may overlook the onset of heatwave events, such as the 2021 Northwest Pacific heatwave, while still capturing the peak stage of heatwaves (Figures S2 and S3 in Supporting Information S1). This discrepancy underscores the importance of including ocean regions in global heatwave analyses.
2. Impact of overlap ratio:
   An insufficient overlap ratio erroneously groups separate regions into a single heatwave event, while an excessive overlap ratio only captures the peak stage of heatwaves, often indicating a quasi-stationary state of the heatwave over land (Figures 2g and 2h), potentially associated with the presence of a heat dome in the region (C. Wang, Zheng, et al., 2022; White et al., 2023). This behavior aligns with the detection of atmospheric blocking, which typically uses a 70% overlap ratio as a criterion (Pfahl et al., 2015; Steinfeld & Pfahl, 2019). An overlap ratio between 40% and 50% strikes a balance, effectively capturing both the onset and peak stages of heatwaves.
3. Role of area and overlap limits:
   Significant discrepancies among the six experiment setups highlight the critical influence of area limit and overlap ratio limit on heatwave detection results at both global and land-only scales. Eliminating the area limit increases the detection of small, localized events driven by local mechanisms rather than atmospheric circulation, decreasing global-scale heatwave metrics. And disregarding the overlap limit causes unrelated heatwave events to merge, reducing global heatwave frequency, duration, and projection area.
4. Minimal influence of resolution and connected structure:
   Our analysis revealed that variations in data resolution and connected structure had minimal impact on the results compared to area and overlap limits.

Unlike previous studies that focused on individual sites or isolated grids (Meehl & Tebaldi, 2004; Perkins, 2015; Perkins et al., 2012), our research provides a robust trend analysis of large-scale contiguous heatwaves over historical period. With continued warming due to anthropogenic forcing expected throughout the twenty-first century (Hansen et al., 2000), we anticipate further increases in heatwave frequency, projection area and total

magnitude. Heatwaves originating over oceans and propagating to land may carry higher moisture content, resulting in humid heatwaves that amplify the impact of humidity on human health (Budd, 2008; Ha et al., 2022; Raymond et al., 2020; Russo et al., 2017). However, the amplifying effects of humidity on heatwaves were not investigated in this study, as our primary focus was on parameters selection for heatwaves identification. Future research should incorporate humidity metrics to better assess the impact of humid heatwaves. Given the profound impact of heatwaves on local economies, human health, and agriculture, investigating the mechanism driving accelerated heatwave trends is crucial for developing effective mitigation and adaptation strategies.

Data Availability Statement

The ERA5 data set is available from Hersbach et al. (2023). All code used to produce the results and figures of this paper is available from the corresponding author upon reasonable request.

Acknowledgments
This work was jointly supported by the National Science Foundation of China (42375021, 42041004). This work was also supported by the Supercomputing Center of Lanzhou University.

References

Barriopedro, D., Fischer, E. M., Luterbacher, J., Trigo, R. M., & García-Herrera, R. (2011). The hot summer of 2010: Redrawing the temperature record map of Europe. *Science*, *332*(6026), 220–224. https://doi.org/10.1126/science.1201224

Barriopedro, D., García-Herrera, R., Ordóñez, C., Miralles, D. G., & Salcedo-Sanz, S. (2023). Heat waves: Physical understanding and scientific challenges. *Reviews of Geophysics*, *61*(2), e2022RG000780. https://doi.org/10.1029/2022rg000780

Bathiany, S., Dakos, V., Scheffer, M., & Lenton, T. M. (2018). Climate models predict increasing temperature variability in poor countries. *Science Advances*, *4*(5), eaar5809. https://doi.org/10.1126/sciadv.aar5809

Budd, G. M. (2008). Wet-bulb globe temperature (WBGT)—Its history and its limitations. *Journal of Science and Medicine in Sport*, *11*(1), 20–32. https://doi.org/10.1016/j.jsams.2007.07.003

Fang, B., & Lu, M. (2020). Heatwave and blocking in the Northeastern Asia: Occurrence, variability, and association. *Journal of Geophysical Research: Atmospheres*, *125*(6), e2019JD031627. https://doi.org/10.1029/2019jd031627

Ha, K.-J., Seo, Y.-W., Yeo, J.-H., Timmermann, A., Chung, E.-S., Franzke, C. L. E., et al. (2022). Dynamics and characteristics of dry and moist heatwaves over East Asia. *Npj Climate and Atmospheric Science*, *5*(1), 49. https://doi.org/10.1038/s41612-022-00272-4

Hansen, J., Sato, M., Ruedy, R., Lacis, A., & Oinas, V. (2000). Global warming in the twenty-first century: An alternative scenario. *Proceedings of the National Academy of Sciences*, *97*(18), 9875–9880. https://doi.org/10.1073/pnas.170278997

He, Y., Zhang, B., Xia, Z., Wang, S., & Guan, X. (2023). Global warming has increased the distance traveled by marine heatwaves. *Geophysical Research Letters*, *50*(2), e2022GL102032. https://doi.org/10.1029/2022gl102032

Hersbach, H., Bell, B., Berrisford, P., Biavati, G., Horányi, A., Muñoz Sabater, J., et al. (2023). ERA5 hourly data on single levels from 1940 to present [Dataset]. *Copernicus Climate Change Service (C3S) Climate Data Store (CDS)*. https://doi.org/10.24381/cds.adbb2d47

King, M. J., & Reeder, M. J. (2021). Extreme heat events from an object viewpoint with application to south-east Australia. *International Journal of Climatology*, *41*(4), 2693–2709. https://doi.org/10.1002/joc.6984

Kjellstrom, T. (2015). Impact of climate conditions on occupational health and related economic losses: A new feature of global and urban health in the context of climate change. *Asia-Pacific Journal of Public Health*, *28*(2_suppl), 28S–37S. https://doi.org/10.1177/1010539514568711

Kong, D., Xie, Y., Gu, X., Slater, L., Ci, H., & Song, H. (2024). Contribution of anthropogenic activities to the intensification of heat index-based spatiotemporally contiguous heatwave events in China. *Journal of Geophysical Research: Atmospheres*, *129*(3), e2023JD040004. https://doi.org/10.1029/2023jd040004

Kornhuber, K., Coumou, D., Vogel, E., Lesk, C., Donges, J. F., Lehmann, J., & Horton, R. M. (2020). Amplified Rossby waves enhance risk of concurrent heatwaves in major breadbasket regions. *Nature Climate Change*, *10*(1), 48–53. https://doi.org/10.1038/s41558-019-0637-z

Kornhuber, K., Osprey, S., Coumou, D., Petri, S., Petoukhov, V., Rahmstorf, S., & Gray, L. (2019). Extreme weather events in early summer 2018 connected by a recurrent hemispheric wave-7 pattern. *Environmental Research Letters*, *14*(5), 054002. https://doi.org/10.1088/1748-9326/ab13bf

Li, J., Wang, Z., Wu, X., Chen, J., Guo, S., & Zhang, Z. (2020). A new framework for tracking flash drought events in space and time. *Catena*, *194*, 104763. https://doi.org/10.1016/j.catena.2020.104763

Lin, H., Mo, R., & Vitart, F. (2022). The 2021 western North American heatwave and its subseasonal predictions. *Geophysical Research Letters*, *49*(6), e2021GL097036. https://doi.org/10.1029/2021gl097036

Liu, Z., & Zhou, W. (2023). Glo3DHydroClimEventSet(v1.0): A global-scale event set of hydroclimatic extremes detected with the 3D DBSCAN-based workflow (1951–2022). *International Journal of Climatology*, *43*(16), 7722–7744. https://doi.org/10.1002/joc.8289

Liu, Z., Zhou, W., & Yuan, Y. (2023). 3D DBSCAN detection and parameter sensitivity of the 2022 Yangtze river summertime heatwave and drought. *Atmospheric and Oceanic Science Letters*, *16*(4), 100324. https://doi.org/10.1016/j.aosl.2022.100324

Lo, S.-H., Chen, C.-T., Russo, S., Huang, W.-R., & Shih, M.-F. (2021). Tracking heatwave extremes from an event perspective. *Weather and Climate Extremes*, *34*, 100371. https://doi.org/10.1016/j.wace.2021.100371

Luo, M., Lau, N. C., Liu, Z., Wu, S., & Wang, X. (2022). An observational investigation of spatiotemporally contiguous heatwaves in China from a 3D perspective. *Geophysical Research Letters*, *49*(6), e2022GL097714. https://doi.org/10.1029/2022gl097714

Luo, M., Wu, S., Lau, G. N.-C., Pei, T., Liu, Z., Wang, X., et al. (2024). Anthropogenic forcing has increased the risk of longer-traveling and slower-moving large contiguous heatwaves. *Science Advances*, *10*(13), eadl1598. https://doi.org/10.1126/sciadv.adl1598

Lyon, B., Barnston, A. G., Coffel, E., & Horton, R. M. (2019). Projected increase in the spatial extent of contiguous US summer heat waves and associated attributes. *Environmental Research Letters*, *14*(11), 114029. https://doi.org/10.1088/1748-9326/ab4b41

McEvoy, D., Ahmed, I., & Mullett, J. (2012). The impact of the 2009 heat wave on Melbourne's critical infrastructure. *Local Environment*, *17*(8), 783–796. https://doi.org/10.1080/13549839.2012.678320

Meehl, G. A., & Tebaldi, C. (2004). More intense, more frequent, and longer lasting heat waves in the 21st century. *Science*, *305*(5686), 994–997. https://doi.org/10.1126/science.1098704

Oertel, A., Pickl, M., Quinting, J. F., Hauser, S., Wandel, J., Magnusson, L., et al. (2023). Everything hits at once: How remote rainfall matters for the prediction of the 2021 North American heat wave. *Geophysical Research Letters*, *50*(3), e2022GL100958. https://doi.org/10.1029/2022gl100958

Osychny, V., & Cornillon, P. (2004). Properties of Rossby waves in the North Atlantic estimated from satellite data. *Journal of Physical Oceanography*, *34*(1), 61–76. https://doi.org/10.1175/1520-0485(2004)034<0061:porwit>2.0.co;2
Perkins, S., & Alexander, L. (2013). On the measurement of heat waves. *Journal of Climate*, *26*(13), 4500–4517. https://doi.org/10.1175/jcli-d-12-00383.1
Perkins, S. E. (2015). A review on the scientific understanding of heatwaves—Their measurement, driving mechanisms, and changes at the global scale. *Atmospheric Research*, *164–165*, 164–165. https://doi.org/10.1016/j.atmosres.2015.05.014
Perkins, S. E., Alexander, L. V., & Nairn, J. R. (2012). Increasing frequency, intensity and duration of observed global heatwaves and warm spells. *Geophysical Research Letters*, *39*(20), L20714. https://doi.org/10.1029/2012gl053361
Perkins-Kirkpatrick, S. E., & Lewis, S. C. (2020). Increasing trends in regional heatwaves. *Nature Communications*, *11*(1), 3357. https://doi.org/10.1038/s41467-020-16970-7
Pfahl, S., Schwierz, C., Croci-Maspoli, M., Grams, C. M., & Wernli, H. (2015). Importance of latent heat release in ascending air streams for atmospheric blocking. *Nature Geoscience*, *8*(8), 610–614. https://doi.org/10.1038/ngeo2487
Raymond, C., Matthews, T., & Horton, R. M. (2020). The emergence of heat and humidity too severe for human tolerance. *Science Advances*, *6*(19), eaaw1838. https://doi.org/10.1126/sciadv.aaw1838
Rousi, E., Kornhuber, K., Beobide-Arsuaga, G., Luo, F., & Coumou, D. (2022). Accelerated western European heatwave trends linked to more-persistent double jets over Eurasia. *Nature Communications*, *13*(1), 3851. https://doi.org/10.1038/s41467-022-31432-y
Rübbelke, D., & Vögele, S. (2011). Impacts of climate change on European critical infrastructures: The case of the power sector. *Environmental Science & Policy*, *14*(1), 53–63. https://doi.org/10.1016/j.envsci.2010.10.007
Russo, E., & Domeisen, D. I. V. (2023). Increasing intensity of extreme heatwaves: The crucial role of metrics. *Geophysical Research Letters*, *50*(14), e2023GL103540. https://doi.org/10.1029/2023GL103540
Russo, S., Sillmann, J., & Sterl, A. (2017). Humid heat waves at different warming levels. *Scientific Reports*, *7*(1), 7477. https://doi.org/10.1038/s41598-017-07536-7
Schumacher, D. L., Hauser, M., & Seneviratne, S. I. (2022). Drivers and mechanisms of the 2021 Pacific northwest heatwave. *Earth's Future*, *10*(12), e2022EF002967. https://doi.org/10.1029/2022ef002967
Song, H., Kong, D., Xiong, L., Gu, X., & Liu, J. (2022). Inter-comparison of diverse heatwave definitions in the analysis of spatiotemporally contiguous heatwave events over China. *Remote Sensing*, *14*(16), 4082. https://doi.org/10.3390/rs14164082
Steinfeld, D., & Pfahl, S. (2019). The role of latent heating in atmospheric blocking dynamics: A global climatology. *Climate Dynamics*, *53*(9–10), 6159–6180. https://doi.org/10.1007/s00382-019-04919-6
Tang, S., Qiao, S., Wang, B., Liu, F., Feng, T., Yang, J., et al. (2023). Linkages of unprecedented 2022 Yangtze River valley heatwaves to Pakistan flood and triple-dip La Niña. *Npj Climate and Atmospheric Science*, *6*(1), 44. https://doi.org/10.1038/s41612-023-00386-3
Vogel, M. M., Zscheischler, J., Fischer, E. M., & Seneviratne, S. I. (2020). Development of future heatwaves for different hazard thresholds. *Journal of Geophysical Research: Atmospheres*, *125*(9), e2019JD032070. https://doi.org/10.1029/2019jd032070
Vogt, L., Burger, F. A., Griffies, S. M., & Frölicher, T. L. (2022). Local drivers of marine heatwaves: A global analysis with an Earth System Model. *Frontiers in Climate*, *4*, 847995. https://doi.org/10.3389/fclim.2022.847995
Wang, C., Zheng, J., Lin, W., & Wang, Y. (2022). Unprecedented heatwave in western North America during late June of 2021: Roles of atmospheric circulation and global warming. *Advances in Atmospheric Sciences*, *40*(1), 14–28. https://doi.org/10.1007/s00376-022-2078-2
Wang, X., Luo, M., Wu, S., Ning, G., Liu, Z., Wang, S., et al. (2022). Spatiotemporal evolution patterns of contiguous extreme precipitation events across China from a 3D perspective. *Geophysical Research Letters*, *49*(16), e2022GL098840. https://doi.org/10.1029/2022gl098840
Wang, Y., & Wang, C. (2023). Classification of extreme heatwave events in the Northern Hemisphere through a new method. *Climate Dynamics*, *61*(3–4), 1947–1969. https://doi.org/10.1007/s00382-022-06649-8
White, R. H., Anderson, S., Booth, J. F., Braich, G., Draeger, C., Fei, C., et al. (2023). The unprecedented Pacific northwest heatwave of June 2021. *Nature Communications*, *14*(1), 727. https://doi.org/10.1038/s41467-023-36289-3
Wu, S., Luo, M., Liu, Z., Wang, X., Huang, Z., & Li, X. (2024). Longer- and slower-moving contiguous heatwaves linked to El Niño. *Geophysical Research Letters*, *51*(11), e2024GL109067. https://doi.org/10.1029/2024gl109067
Xu, Z., FitzGerald, G., Guo, Y., Jalaludin, B., & Tong, S. (2016). Impact of heatwave on mortality under different heatwave definitions: A systematic review and meta-analysis. *Environment International*, *89–90*, 89–90. https://doi.org/10.1016/j.envint.2016.02.007
Ye, X., Wolff, R., Yu, W., Vaneckova, P., Pan, X., & Tong, S. (2012). Ambient temperature and morbidity: A review of epidemiological evidence. *Environmental Health Perspectives*, *120*(1), 19–28. https://doi.org/10.1289/ehp.1003198
Zander, K. K., Botzen, W. J. W., Oppermann, E., Kjellstrom, T., & Garnett, S. T. (2015). Heat stress causes substantial labour productivity loss in Australia. *Nature Climate Change*, *5*(7), 647–651. https://doi.org/10.1038/nclimate2623